J|A|C|S
ARTICLES
Published on Web 03/06/2004

# Electrocatalytic Activity of Ordered Intermetallic Phases for Fuel Cell Applications

Emerilis Casado-Rivera,† David J. Volpe,† Laif Alden,† Cora Lind,† Craig Downie,† Terannie Vázquez-Alvarez,† Antonio C. D. Angelo,‡ Francis J. DiSalvo,*,† and Héctor D. Abruña*,†

*Contribution from the Department of Chemistry & Chemical Biology, Baker Laboratory, Cornell University, Ithaca, New York 14853-1301, and Laboratory Electrocatalise, P. O. Box 473, Bauru, São Paulo, Brazil*

Received September 12, 2003; E-mail: hda1@cornell.edu (H.D.A); fjd3@cornell.edu (F.J.D.).

***Abstract:*** The electrocatalytic activities of a wide range of ordered intermetallic phases toward a variety of potential fuels have been studied, and results have been compared to those of a pure polycrystalline platinum ($Pt_{pc}$) electrode. A significant number of the ordered intermetallic phases exhibited enhanced electrocatalytic activity when compared to that of Pt, in terms of both oxidation onset potential and current density. The PtBi, PtIn, and PtPb ordered intermetallic phases appeared to be the most promising electrocatalysts tested thus far for fuel cell applications. PtPb, in particular, showed an onset potential that was 100 mV less positive and a peak current density ~40 times higher than those observed for Pt in the case of methanol oxidation. The ability to control the geometric and electronic structures of the electrocatalytic material by using ordered intermetallic phases has been shown to be a promising direction of inquiry in the search for superior electrocatalysts for fuel cell applications.

## Introduction

In the last two decades, interest in the direct conversion of chemical energy to electricity, via a fuel cell, has surged for a range of applications. In transportation, fuel cell use would circumvent Carnot cycle limitations and can, in principle, supply energy with an efficiency in excess of 80%,[1] depending on the fuel used. For more compact applications, fuel cells could replace static energy sources, such as Li-ion batteries, providing longer lifetimes and higher energy densities.[1] As its oxidation is mechanistically easiest, hydrogen is often seen as a likely fuel for fuel cells. So-called $H_2/O_2$ fuel cells, however, require either on-site $H_2$ storage or an onboard reformer to extract $H_2$ from organic fuels. Steam reformation is a high-temperature (~650 °C, depending on the fuel)[1,2] method where the fuel is combined with water to form carbon dioxide, carbon monoxide, and hydrogen, which must then be purified before introduction into the fuel cell. Such high temperature requirements generally limit steam reformers to use in large fixed installations that use solid oxide fuel cells (SOFC). At lower temperatures, catalytic partial oxidation, or so-called air reformers, can be used.[3] This method combines oxygen directly from air with the fuel to produce $CO_2$ and $H_2$. While this method can be employed at lower temperatures (very recently reported to be as low as 350 °C for methanol by Krumpelt et al. at Argonne National Lab, U.S. Patent 6,244,367), noble metal catalysts are required, and a significant amount of chemical energy is necessarily lost in the process (more than 30% of the free energy of combustion is lost for methanol in the nonelectrolytic formation of $CO_2$). In addition, these reformer temperatures are still too high for many smaller applications or for uses that require short induction periods, for which fuel cells would be otherwise well-suited.

As such, there has been a drive to study the direct electrocatalytic oxidation of small organic molecules (SOMs) for potential use as fuels in so-called direct fuel cells. Primarily, single carbon containing (C-1) compounds have been studied, such as formic acid and methanol, as they have relatively clean oxidative pathways. More complex fuels, such as ethanol, are also attractive, because of their higher energy density, lower toxicity, and greater availability. Ethanol is also particularly attractive because it is a biogenerated fuel, and it does not release carbon that was previously sequestered underground as coal, petroleum, or natural gas into the atmosphere.

The oxidation of any fuel requires the use of a catalyst to achieve the current densities required for practical applications, and platinum-based catalysts are some of the most efficient materials for the oxidation of SOMs. While Pt is an excellent catalyst for the dehydrogenation of fuels, most candidate fuels also require the catalytic surface to be an oxygen source to enact complete oxidation to carbon dioxide. Platinum is extremely susceptible to poisons such as thiols and CO, which is often an intermediate (typically from dissociative chemisorption of the fuel) of such reactions. These poisons remain strongly adsorbed,

† Cornell University.
‡ Laboratory Electrocatalise.

(1) Lamy, C. L.; J.-M; Srinivasan, S. *Direct Methanol Fuel Cells: From a Twentieth Century Electrochemist's Dream to a Twenty-first Century Emerging Technology*; Kluwer Academic/Plenum Publishers: New York, 2001; Vol. 34.
(2) Discussions with Dr. Michael Badding, Corning Inc.
(3) Ahmed, S.; Krumpelt, M.; Kumar, S. H. D.; Lee, J. D.; Carter, R.; Wilkenhoener, R.; Marshall, C. In *1998 Fuel Cell Seminar*; Palm Springs, CA, 1998.

10.1021/ja038497a CCC: $27.50 

especially at bridging and 3-fold hollow sites, and block the surface's active sites from further catalysis, resulting in a dramatic decrease in efficiency.

To mitigate poisoning, Pt-based alloys, particularly PtRu, have been used as bifunctional catalysts, where the platinum activates the fuel to dehydrogenation and the other metal(s) provides the necessary oxygen for complete oxidation of the fuel to $CO_2$. Indeed, PtRu alloys have shown relative tolerance to CO poisoning, increased current densities, and a decreased overpotential for fuel oxidation[4−7] when compared to pure platinum. In fact, PtRu remains the industry and research standard, and in recent years, the primary direction of fuel cell anode development has been in the enhancement of PtRu-based systems. As such, the materials employed as anodes have remained virtually unchanged but have been better engineered to improve performance.[1,8] Such efforts include important advances in making small particles of the electrocatalysts,[9,10] in refining the composition of the catalyst,[11−13] and in surface structure elucidation of the purported active form of the catalysts.[8,14,15] However, even PtRu still suffers from a significant overpotential for the oxidation of organic fuels and from poisoning by sulfur-containing compounds, each of which results in loss of catalytic efficiency. Furthermore, as with all alloys, PtRu has an inherently poorly defined surface structure, with its surface sites occupied by Pt or Ru in a random, uncontrolled fashion. In addition, the use of Ru-based alloys in place of pure Pt introduces a stability problem: during extended periods of operation, particularly under non-optimal usage (especially at high temperature and current density), the alloy surface becomes depleted of Ru.[16,17] In some cases, Ru has been reported to nucleate in other parts of the cell and to facilitate degradation of the membrane[16] that separates the anode and the cathode. This breakdown of the membrane allows fuel crossover to the cathode, which further diminishes efficiency.

A number of other materials, besides PtRu, have been recently studied for fuel cell applications. Of these materials, PtSn has been one of the most widely studied, although there are some discrepancies in terms of which form, the alloy or Sn deposited on Pt, is or is supposed to be the most active material toward the oxidation of methanol.[18,19] Other studies have looked at different binary alloys of Pt and metals, such as Mo, W, Re, Rh, and Pd.[20] More complex alloys including ternary and quaternary have also been explored as fuel cell electrocatalysts.[13] Previously we reported[21] on a new approach in the search for electrocatalysts to supplant PtRu with less expensive alternatives and to circumvent the inherent problems of alloys as catalysts. In that study, in place of an alloy, an ordered intermetallic phase, PtBi, was studied as a candidate for formic acid oxidation. The choice of PtBi was based on the known electrocatalytic activity of Pt surfaces modified with irreversibly adsorbed Bi adlayers.[22−26]

Ordered intermetallic systems, in general, provide predictable control over structural, geometric, and electronic effects not afforded by alloys. Further, as the order in intermetallic phases arises from the high enthalpy of mixing, a higher chemical and structural stability than found in disordered alloys, such as PtRu, can be expected. Unlike alloys, which have varying surface composition and thus randomly distributed active sites, on a given PtBi surface, all Pt (and Bi) atoms have the same local geometry and thus the same activity. Further, in any Pt-based alloy, the Pt−Pt distance for nearest-neighbor Pt atoms is essentially the same as in Pt metal (2.78 Å). In ordered intermetallic compounds the Pt−Pt distances can be modulated over a range of a factor of 2. For example, in PtBi the Pt−Pt distance in the (001) plane is 4.32 Å. Such distances were expected to significantly mitigate CO poisoning, by reducing bridge sites and eliminating 3-fold hollow adsorption sites. Indeed, PtBi displayed virtual immunity to CO poisoning, and compared to pure Pt, both a dramatically enhanced current density for formic acid oxidation and a shift in the onset of oxidation potential of approximately 300 mV less positive.[21]

These results have prompted research, described herein, into the electrocatalytic oxidation by PtBi of other SOMs, namely, methanol, ethanol, ethylene glycol, and acetic acid. In addition, we report on a broad range of other Pt-based intermetallic phases, $PtBi_2$, PtIn, $PtIn_2$, $Pt_3In_7$, PtPb, PtMn, PtSb, $PtSb_2$, PtSn, $PtSn_2$, $PtSn_4$, $Pt_2Sn_3$, and $Pt_3Sn$, examined as potential catalysts for the oxidation of fuels for fuel cell applications. Whereas $Pt_3Sn$ has also been studied, it exhibited minimal activity as electrocatalyst for fuel cell applications.[27,28] Finally, we examine the activity of non-Pt-based intermetallic compounds: PdBi and PdSb.

## Experimental Section

The preparation and characterization of the PtBi intermetallic phase were described previously.[21] The other intermetallic phases were obtained through the following procedure. For $PtBi_2$, PtPb, PtIn, $PtIn_2$, $Pt_3In_7$, $PtSn_2$, $PtSn_4$, PtSb, PdBi, and PdSb, stoichiometric amounts of granular platinum and the appropriate second metal were sealed under vacuum in a quartz tube. Typically, the sample was then heated (see Table 1 for temperatures) in a box furnace and held for 9−12 h at that temperature before being quenched to room temperature. The sample was ground with an agate mortar and pestle, and an X-ray diffraction

(4) Costamanga, P.; Srinivisan, S. *J. Power Sources* **2001**, *102*, 242−252.
(5) Schmidt, T. J.; Gasteiger, H. A.; Behm, R. J. *J. Electrochem. Soc.* **1999**, *146*, 1296.
(6) Narayanan, S. R.; Chun, W.; Valdez, T. I.; Jeffries-Nakamura, B.; Frank, H.; Surampudi, S.; Halpert, G.; Kosek, J.; Cropley, C.; LaConti, A. B.; Smart, M.; Wang, Q. J.; Prakash, G. S.; Olah, G. In *Fuel Cell Seminar*; Orlando, FL, 1996; p 525.
(7) Ren, X.; Zelenay, P.; Thomas, S.; Davey, J.; Gottesfield, S. *J. Power Sources* **2000**, *86*, 111.
(8) Costamanga, P.; Srinivisan, S. *J. Power Sources* **2001**, *102*, 253−269.
(9) Gasteiger, H. A.; Markovic, N. M.; Ross, P. N. *J. Phys. Chem.* **1995**, *99*, 8290−8301.
(10) Long, J. W.; Stroud, R. M.; Swider-Lyons, K. E.; Rolison, D. R. *J. Phys. Chem. B* **2000**, *104*, 9772−9776.
(11) Lee, C. E.; Tiege, P. B.; Zing, Y.; Nagendran, J.; Bergens, S. H. *J. Am. Chem. Soc.* **1997**, *119*, 3543.
(12) Lee, C. E.; Bergens, S. H. *J. Electrochem. Soc* **1998**, *145*, 4182.
(13) Mallouk, T. E.; Smotkin, E. S.; Reddington, E.; Sapienza, A.; Lafrenz, T. J.; Chan, B. C.; Gurau, B.; Viswanathan, R.; Liu, R.; Sarangapani, S.; Ley, K. L. *J. Phys. Chem. B* **1998**, *102*, 9997−10003.
(14) Chrzanowski, W.; Wieckowski, A. *Langmuir* **1998**, *14*, 1967−1970.
(15) Chrzanowski, W.; Wieckowski, A. *Langmuir* **1997**, *13*, 5974−5978.
(16) Private communication, Dr. Grant Ehrlich, UTC Fuel Cells.
(17) Private communication, Dr. Shimshon Gottesfeld, MTI Micro Fuel Cells.
(18) Wang, K.; Gasteiger, H. A.; Markovic, N. M.; Ross, P. N. *Electrochim. Acta* **1996**, *41*, 2587.
(19) Wasmus, S.; Küver, A. *J. Electroanal. Chem.* **1999**, *461*, 14−31.
(20) Hogarth, M. P.; Ralph, T. R. *Platinum Metals Rev.* **2002**, *46*, 146.
(21) Casado Rivera, E.; Gál, Z.; Angelo, A. C. D.; Lind, C.; DiSalvo, F. J.; Abruña, H. D. *Chem. Phys. Chem.* **2003**, *4*, 193−199.
(22) Smith, S. P. E.; Abruna, H. D. *J. Electroanal. Chem.* **1999**, *467*, 43−49.
(23) Smith, S. P. E.; Ben-Dor, K. F.; Abruna, H. D. *Langmuir* **1999**, *15*, 7325−7332.
(24) Smith, S. P. E.; Ben-Dor, K. F.; Abruna, H. D. *Langmuir* **2000**, *16*, 787−794.
(25) Clavilier, J.; Fernandez-Vega, A.; Feliu, J. M.; Aldaz, A. *J. Electroanal. Chem.* **1989**, *261*, 113−125.
(26) Clavilier, J.; Fernandez-Vega, A.; Feliu, J. M.; Aldaz, A. *J. Electroanal. Chem* **1989**, *258*, 89−100.
(27) Ross, P. N.; Markovic, N. M.; Stamenkovic, V. R.; Arenz, M.; Lucas, C. A.; Gallagher, M. E. *J. Am. Chem. Soc.* **2003**, *125*, 2736−2745.
(28) Hayden, B. E.; Rendall, M. E.; South, O. *J. Am. Chem. Soc.* **2003**, *125*, 7738−7742.

***Table 1.*** Preparation Temperature for Intermetallic Phases

| intermetallic phase | temp (°C) |
|---|---|
| $PtBi_2$ | 735 |
| PtPb | 875 |
| PtIn | 1100 |
| $PtIn_2$ | 1100 |
| $Pt_3In_7$ | 1100 |
| $PtSn_2$ | 1100 |
| $PtSn_4$ | 850 |
| PtSb | 1150 |
| PdBi | 850 |
| PdSb | 850 |

(XRD) powder pattern was taken to confirm the composition of the intermetallic phase. The annealing procedure was repeated, without grinding, to cast the sample into a suitable bulk electrode. To eliminate porosity, the molten sample was periodically shaken to remove gases. Samples that exhibit peritectic decomposition typically needed to be annealed below the decomposition temperature for up to several days to achieve phase purity. For other, more refractory materials (PtMn, $Pt_3Sn$, $Pt_2Sn_3$, PtSn, and $PtSb_2$), stoichiometric amounts of platinum and the appropriate second metal were pressed into a pellet in a pellet press and arc-melted, forming a metallic button. This button was then cast into an electrode slug in a graphite crucible in an RF furnace. The sample was ground with an agate mortar and pestle, and an XRD powder pattern was taken to confirm the composition of the intermetallic phase. The annealing procedure was repeated, without grinding, to cast the sample into a suitable bulk electrode.

In most cases, the resulting pellets were cut into cylinders of ca. 3−5 mm in length and either 3 or 7 mm in diameter. The procedure used to mount these pellets was described previously.[21] In cases where it was not possible to get a cylinder, the droplike shaped piece of material was polished following the same procedure used for the pellets[21] and then welded to a platinum or silver wire with tin solder (this connection was covered with Teflon tape). For this kind of electrode, the resistance was less than 0.5 Ω and the electrochemical studies were performed using the hanging meniscus technique.

Prior to each experiment, electrodes were polished with diamond paste (METADI−Buehler, $\phi = 1\ \mu$m) and rinsed with Millipore water (18 MΩ·cm, Millipore Milli-Q). In most cases, after being polished with diamond paste, the electrode was cycled in the supporting electrolyte until a stable cyclic voltammogram was obtained (∼10 min at 50 or 10 mV/s) prior to the oxidation of the fuel. This and other surface treatments prior to electrochemical oxidation of the fuels were discussed in detail previously.[29] The cyclic voltammograms for the oxidation of the fuels were recorded at a sweep rate of 10 mV/s, unless otherwise noted. All the solutions were prepared with Millipore water. Solutions of 0.1 M sulfuric acid (J. T. Baker ultrapure reagent) were used as supporting electrolyte. In some cases perchloric acid (Aldrich Chemical Co. Inc., $HClO_4$ redistilled 99.999% $HClO_4$ content 69.0−72.0%) was used as supporting electrolyte instead of sulfuric acid. Formic acid (Fisher Chemical, 88% certified ACS), methanol (Mallinckrodt analytical reagent, anhydrous meets ACS specifications 99.9%), ethanol (Pharmacoproducts Inc., 200 proof ACS/USP grade), ethylene glycol (Mallinckrodt analytical reagent, acidity 0.001%) and acetic acid (Alfa Aesar−Johnson Matthey, glacial 99.9985%) solutions were also used (as received) in our studies. All solutions were deaerated with prepurified nitrogen for at least 10 min, and measurements were conducted at room temperature. All potentials are referenced to a saturated Ag/AgCl electrode without regard for the liquid junction.

## Results

**Oxidation of the Electrode Surface.** Figure 1 shows the cyclic voltammograms (CVs) obtained for selected electrode materials in a 0.1 M sulfuric acid solution. While the Pt electrode (Figure 1a) displayed the typical hydrogen adsorption/desorption peaks, as well as well-defined surface oxidation and reduction peaks (onset of oxidation at +0.56 V), the intermetallic electrodes typically (Figure 1b shows a representative example) showed very little, if any, evidence of hydrogen adsorption/desorption.

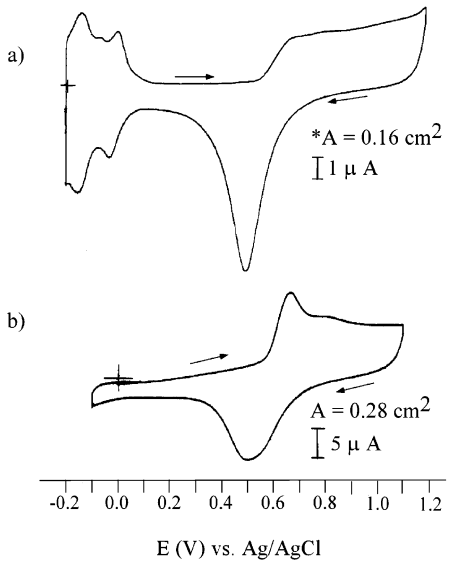


***Figure 1.*** Cyclic voltammograms obtained for selected electrode materials in a 0.1 M sulfuric acid solution for (a) Pt and (b) PtPb, both recorded at a sweep rate of 10 mV/s. $A$ = geometric surface area.

***Table 2.*** Onset of Surface Oxidation in 0.1 M $H_2SO_4$

| electrode material | onset of surface oxidation[a] (V) |
|---|---|
| Pt | +0.56 |
| PtBi | +0.50 |
| PdBi | +0.63 |
| PtPb | +0.55 |
| PtSn | +0.40 |
| $Pt_3Sn$ | +0.33 |
| PtSb | +0.47 |
| PtMn | +0.40 |

[a] In 0.1 M $H_2SO_4$ at a sweep rate of 10 mV/s.

They did all, however, exhibit an oxidation wave in the potential range of +0.4 to +0.6 V, which has been ascribed to surface oxide formation. The onset of surface oxidation tended to be shifted negative in the intermetallics' CVs, compared to that of pure Pt. Because it is widely believed that the presence of oxygenated species at the surface is critical to the oxidation of candidate fuels, these shifts are noteworthy and are summarized in Table 2.

A number of other electrode materials were tested in 0.1 M $HClO_4$. The choice of acid used as electrolyte was guided by the stability of the intermetallic in each acid. For instance, it was found that PtIn was unstable in $H_2SO_4$ at positive potentials and it was thus studied in $HClO_4$. In fact, $Pt_3In_7$, $PtSn_2$, and $PtSn_4$ were determined to be unstable both in sulfuric acid and in perchloric acid and were not investigated further. Figure 2 shows the cyclic voltammograms obtained for Pt, PtBi, and PtIn in a 0.1 M perchloric acid solution. Again, Pt (Figure 2a) showed well-defined surface oxidation and hydrogen adsorption/desorption peaks. Meanwhile, the CVs of the intermetallic phases (Figure 2b,c) had fewer features, lacking strong indication of

(29) Volpe, D. J.; Casado Rivera, E.; Alden, L.; Lind, C.; Haggerdon, K.; Downie, C.; Korzeniewski, C.; Abruña, H. D.; DiSalvo, F. J. *J. Electrochem. Soc.* **2003**, in press.

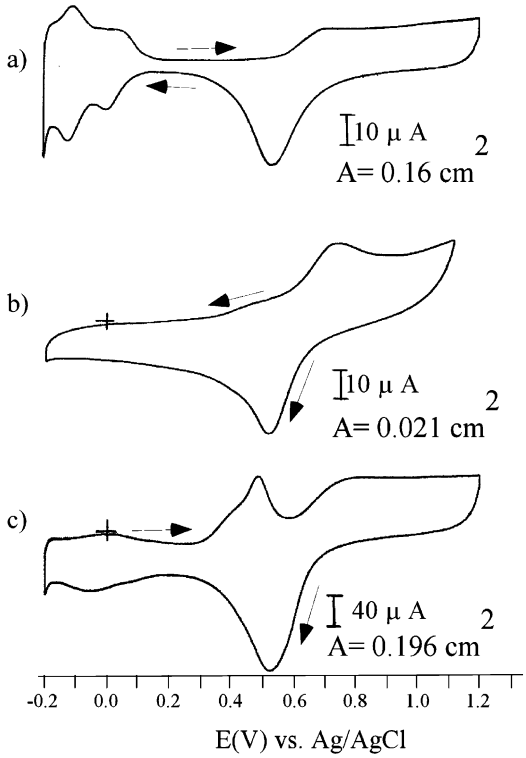


***Figure 2.*** Cyclic voltammograms obtained for selected electrode materials in a 0.1 M perchloric acid solution: (a) Pt, (b) PtBi, and (c) PtIn, all recorded at a sweep rate of 10 mV/s.

***Table 3.*** Onset of Surface Oxidation in 0.1 M $HClO_4$

| electrode material | onset of surface oxidation[a] (V) |
|---|---|
| Pt | +0.56 |
| PtBi | +0.56 |
| PtIn | +0.35 |
| $Pt_3Sn$ | +0.10 |
| $Pt_2Sn_3$ | +0.30 |
| PtSb | +0.25 |
| PdSb | +0.56 |

[a] In 0.1 M $HClO_4$ at 10 mV/s.

hydrogen adsorption, and with far broader surface oxidation peaks. Data are summarized in Table 3.

While the Sn-containing intermetallics displayed a dramatic negative shift in the onset of surface oxidation potential, these peaks were rather poorly defined and partially obscured by a large ohmic current; thus the above values are presented with caution.

**Formic Acid Oxidation.** It was hoped that formic acid could be used as an effective initial screen for candidate electrode materials. Mechanistically, formic acid can act as a model system for more complex oxidation pathways, such as those for methanol and ethanol. Unlike ethanol, however, C−C bond cleavage is not necessary, nor does additional oxygen need to be provided to generate $CO_2$, as would be the case for both methanol and ethanol. Thus, it is believed that any electrode that is active for either methanol or ethanol should show pronounced activity for formic acid.

Figure 3 depicts representative CVs of a number of electrode materials active in the oxidation of formic acid. Electrodes composed of $PtIn_2$, $PtSb_2$, PdBi, and PdSb were also tested but were found to be inactive toward formic acid oxidation, and thus are not shown. In fact, these materials were also found to

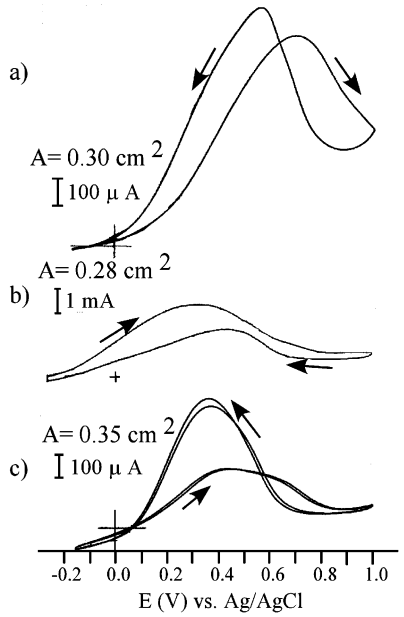


***Figure 3.*** Representative cyclic voltammograms at 10 mV/s for PtIn, PtPb, and PtSn toward the oxidation of formic acid: (a) PtIn, 0.1 M $HClO_4$/0.125 M HCOOH; (b) PtPb, 0.1 M $H_2SO_4$/0.25 M HCOOH; (c) PtSn, 0.1 M $H_2SO_4$/0.5 M HCOOH.

***Table 4.*** Formic Acid Oxidation on Different Intermetallic Phases

| electrode | electrolyte | formic acid concn (M) | onset of oxidation potential (mV) | peak current potential (mV) | peak current density ($\mu$A/cm$^2$) |
|---|---|---|---|---|---|
| Pt | $H_2SO_4$ | 0.25 | 150 | 680 | 220 |
| Pt | $HClO_4$ | 0.125 | 120 | 650 | 500 |
| PtBi | $HClO_4$ | 0.125 | 160 | 555 | 3800 |
| PtBi[a] | $H_2SO_4$ | 0.125 | −125 | 550 | 2400 |
| $PtBi_2$[b] | $H_2SO_4$ | 0.5 | 210 | 750 | 24 000 |
| PtPb | $H_2SO_4$ | 0.25 | −150 | 260 | 8200 |
| PtIn | $HClO_4$ | 0.125 | 50 | 500 | 930 |
| PtMn | $H_2SO_4$ | 0.125 | 100 | 400 | 40 |
| PtSn | $H_2SO_4$ | 0.5 | 60 | 380 | 630 |
| $Pt_3Sn$ | $H_2SO_4$ | 0.25 | 0 | 480 | 480 |
| $Pt_3Sn$ | $HClO_4$ | 0.25 | 100 | 380 | 350 |
| $Pt_2Sn_3$ | $H_2SO_4$ | 0.5 | −100 | 440 | 470 |
| $Pt_2Sn_3$ | $HClO_4$ | 0.125 | c | 430 | 20 |
| PtSb | $H_2SO_4$ | 0.5 | −70 | 310 | 890 |
| PtSb | $HClO_4$ | 0.25 | 0 | 260 | 100 |

[a] Summarized results of previously published data, for comparison. [b] Due to significant bubble formation, presumably $CO_2$, this electrode was rotated at 2000 rpm in an RDE configuration. [c] This value could not be determined.

be inactive toward all fuels tested (formic acid, methanol, ethanol, ethylene glycol, and acetic acid), thus supporting the contention that formic acid can be a useful initial screen. Results for electrodes active toward formic acid oxidation are summarized in Table 4; note that all values refer only to the anodic sweep of each CV, with a sweep rate of 10 mV/s.

Of the materials tested, PtBi, $PtBi_2$, PtPb, and PtIn showed the most promising results. Upon cycling, each produced bubbles concomitant with the onset of anodic current, suggesting that formic acid was completely oxidized to $CO_2$. In fact, PtPb showed an onset of oxidation potential of approximately 300 mV less positive than pure Pt. While all current densities reported in this paper were calculated with respect to geometric surface area (GSA), and there was likely some degree of roughness associated with each electrode, all materials displayed a mirror finish upon polishing, which was still evident after cycling. Thus, it was highly unlikely that the enhanced current

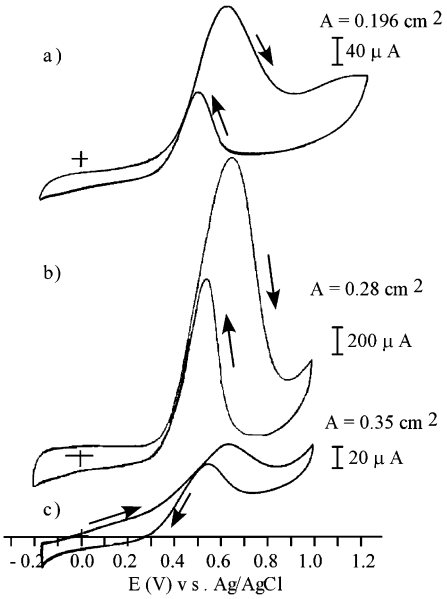


***Figure 4.*** Cyclic voltammograms of a number of electrode materials active toward the oxidation of methanol: (a) PtIn, 0.1 M $HClO_4$/0.125 M methanol at 10 mV/s; (b) PtPb, 0.1 M $H_2SO_4$/0.2 M methanol at 10 mV/s; (c) PtSn, 0.1 M $H_2SO_4$/0.5 M methanol at 10 mV/s.

***Table 5.*** Results Obtained for the Oxidation of Methanol on Different Intermetallic Phases

| electrode | electrolyte | methanol concn (M) | onset of oxidation potential (mV) | peak current potential (mV) | peak current density ($\mu$A/cm$^2$) |
|---|---|---|---|---|---|
| Pt | $H_2SO_4$ | 0.25 | 390 | 640 | 210 |
| Pt | $HClO_4$ | 0.25 | 370 | 570 | 400 |
| PtPb | $H_2SO_4$ | 0.2 | 290 | 630 | 8000 |
| PtIn | $HClO_4$ | 0.125 | 330 | 610 | 1100 |
| PtSn | $H_2SO_4$ | 0.5 | 300 | 600 | 110 |
| PtSb | $H_2SO_4$ | 0.25 | 430 | 620 | 40 |

densities displayed by a number of the intermetallic electrodes (a factor of 40, in the case of PtPb) were primarily due to surface area discrepancies, but rather they were due to significant increases in specific activity. In fact, the Pt electrode used for comparison was prepared and cleaned by the same procedure that was used for the intermetallic electrodes, and hence it likely had comparable surface roughness.

**Methanol Oxidation.** Next, each intermetallic material was tested as an electrocatalyst for methanol oxidation. Figure 4 depicts the CVs of PtIn, PtPb, and PtSn toward the oxidation of methanol. The PtBi, $PtBi_2$, PtMn, $Pt_2Sn_3$, and $Pt_3Sn$ ordered intermetallic phases, all of which exhibited varying levels of activity toward formic acid oxidation, did not appear to activate methanol to electrooxidation. Representative cyclic voltammograms are displayed in Figure 4, and results of the initial anodic sweeps are summarized in Table 5. Not surprisingly, all active electrodes showed a significant positive shift in onset of oxidation, owing to the relative difficulty in oxidizing methanol compared to formic acid. As mentioned earlier, in this case, the catalyst must provide oxygen to the fuel to generate $CO_2$, in addition to dehydrogenating the fuel. However, most intermetallic phases demonstrated decidedly better activity than pure Pt, with an onset of oxidation potential 100 mV less positive for PtPb. The PtIn and PtPb electrodes also displayed high current densities, similar to the values they displayed for formic acid oxidation. The current density of PtIn was approximately

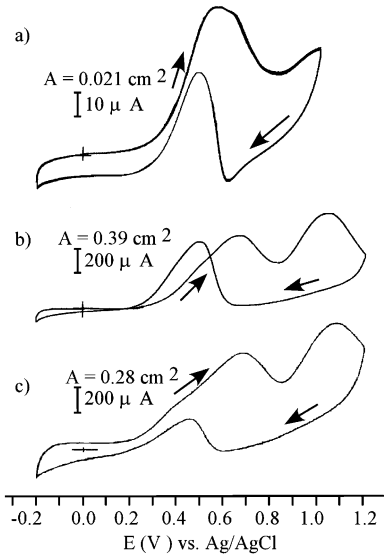


***Figure 5.*** Cyclic voltammograms at 10 mV/s for PtBi, PtIn, and PtPb toward the oxidation of ethanol: (a) PtBi, 0.1 M $HClO_4$/0.125 M ethanol; (b) PtIn, 0.1 M $HClO_4$/0.125 M ethanol; (c) PtPb, 0.1 M $H_2SO_4$/0.5 M ethanol.

***Table 6.*** Results Obtained for the Oxidation of Ethanol on Different Intermetallic Phases

| electrode | electrolyte | ethanol concn (M) | onset of oxidation potential (mV) | peak current potential (mV) | peak current density ($\mu$A/cm$^2$) |
|---|---|---|---|---|---|
| Pt | $H_2SO_4$ | 0.25 | 370 | 680 | 130 |
| Pt | $HClO_4$ | 0.125 | 250 | 640 | 860 |
| PtBi | $HClO_4$ | 0.125 | 320 | 560 | 2200 |
| PtPb | $H_2SO_4$ | 0.25 | 130 | 660 | 3000 |
| PtIn | $HClO_4$ | 0.125 | 280 | 650 | 1300 |
| PtMn | $H_2SO_4$ | 0.125 | 200 | 650 | 200 |
| PtSn | $H_2SO_4$ | 0.5 | 100 | 390 | 75 |
| PtSb | $H_2SO_4$ | 0.5 | 240 | 520 | 63 |

3 times that of pure Pt, while PtPb had a current density more than 40 times as great as Pt.

**Ethanol Oxidation and Acetic Acid Oxidation.** Ethanol is also a potential fuel of interest for fuel cell applications. The $PtBi_2$, $Pt_2Sn_3$, and $Pt_3Sn$ intermetallic phases were found to be inactive toward ethanol oxidation. Interestingly, both PtBi and PtMn, which were inactive toward methanol oxidation, exhibited significant ability to oxidize ethanol. Why this may be is presently the subject of investigation. Representative cyclic voltammograms are shown in Figure 5, and the results from active materials are summarized in Table 6. While measurements of peak current were limited to the oxidation wave at ca. 0.6 V for each material, a second oxidation wave was visible at between 1.0 and 1.1 V. At this time, the nature of the redox processes at each of these potentials is unclear, but it is posited that none of these materials oxidized ethanol completely to $CO_2$ at low potentials, instead generating only intermediates (likely including acetic acid) as C−C bond cleavage is likely the most mechanistically difficult step. To explore this, all electrodes were tested for activity toward acetic acid oxidation (see Figure 6 for example). That none of these materials (including pure Pt) was active toward the oxidation of acetic acid supports this claim, and further characterization of electrooxidation intermediates via in situ Fourier transform infrared spectroscopy (FT-IR) supported this hypothesis and will be discussed in a forthcoming publication. Nevertheless, once again, of all

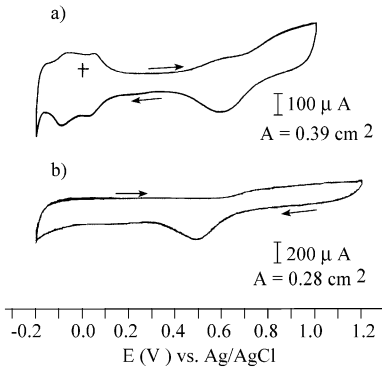


***Figure 6.*** Representative cyclic voltammograms at 10 mV/s for the oxidation of acetic acid: (a) PtIn, 0.1 M $HClO_4$/0.125 M acetic acid; (b) PtPb, 0.1 M $H_2SO_4$/0.125 M acetic acid.

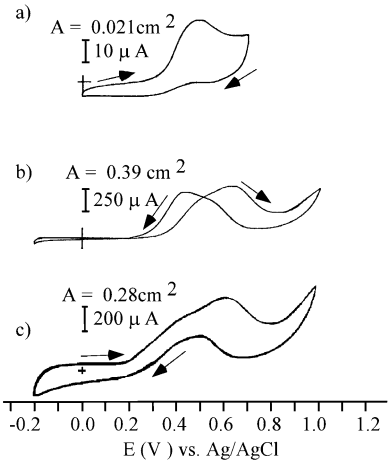


***Figure 7.*** Representative cyclic voltammograms at 10 mV/s for the oxidation of ethylene glycol: (a) PtBi, 0.1 M $HClO_4$/0.125 M ethylene glycol; (b) PtIn, 0.1 M $HClO_4$/0.125 M ethylene glycol; (c) PtPb, 0.1 M $H_2SO_4$/0.25 M ethylene glycol.

***Table 7.*** Results Obtained for the Oxidation of Ethylene Glycol on Different Intermetallic Phases

| electrode | electrolyte | ethylene glycol concn (M) | onset of oxidation potential (mV) | peak current potential (mV) | peak current density ($\mu$A/cm$^2$) |
|---|---|---|---|---|---|
| Pt | $H_2SO_4$ | 0.25 | 270 | 630 | 320 |
| Pt | $HClO_4$ | 0.125 | 480 | 620 | 300 |
| PtBi | $HClO_4$ | 0.125 | 310 | 480 | 810 |
| PtPb | $H_2SO_4$ | 0.25 | 160 | 590 | 1900 |
| PtIn[a] | $HClO_4$ | 0.125 | 310 | 630 | 960 |
| PtSn | $H_2SO_4$ | 0.5 | 140 | 320 | 23 |
| PtSb | $H_2SO_4$ | 0.5 | 315 | 560 | 34 |

[a] Sweep rate: 30 mV/s.

electrodes tested, PtPb showed both a greater negative shift in onset of oxidation potential and a substantially higher current density, both compared to pure Pt.

**Ethylene Glycol Oxidation.** Finally, the electrode materials were tested with ethylene glycol as a potential fuel for electrooxidation. Figure 7 depicts the CVs of PtBi, PtIn, and PtPb toward the oxidation of ethylene glycol. Again, $PtBi_2$, $Pt_2Sn_3$, and $Pt_3Sn$ were not active, while PtMn (which was active toward ethanol but not methanol) also showed no activity. Results are summarized in Table 7. As previously seen for other fuels, each active intermetallic material displayed both enhanced current densities and onset of oxidation potentials far better than those of pure Pt. In particular, PtPb showed a 110 mV negative shift in its oxidation wave and a current density 6 times that of Pt. As with ethanol, however, it was unclear for any of these materials whether the fuel was completely oxidized to $CO_2$ until significantly more positive potentials than shown above were reached or whether a partially oxidized species was generated. Preliminary differential electrochemical mass spectrometry (DEMS) results (unpublished) for the oxidation of ethylene glycol on PtBi indicate that the latter might be true, since no CO or $CO_2$ was detected. However, this aspect is still under investigation.

## Conclusions

The electrocatalytic activities of a wide range of ordered intermetallic phases toward a variety of potential fuels have been studied, and results have been compared to those of a pure Pt electrode, prepared in an identical manner. A significant number of the ordered intermetallic phases exhibited electrocatalytic activity superior to that of pure polycrystalline Pt in terms of both potential of onset of oxidation and current density. The use of ordered intermetallic phases has thus been shown to offer a viable avenue of research in the quest to find suitable electrocatalysts for fuel cell applications. Several particularly promising candidates, such as PtBi, PtPb, and PtIn, are presently the objects of further characterization by means of FT-IR and DEMS for the identification of intermediates and product distributions. In addition, the electrocatalytic activity of the most promising materials is being studied at higher temperatures to determine their practicality under more realistic fuel cell operating conditions. A comparison study between PtRu and the most promising intermetallic phases with micrometer-sized particles and nanoparticles is also being conducted to determine how competitive these materials would be as fuel cell catalysts.

In addition, based on the work shown here, a number of broad generalizations can be made to accelerate the search for superior electrocatalysts from the myriad of intermetallic phases available. It has been shown that, of the materials examined here, only Pt-containing intermetallic phases have shown any activity. This finding, while too soon to be conclusive, is not surprising, because of all elements, Pt excels at catalysis of dissociative chemisorption of SOMs, which is believed to be the initial step in electrooxidation. For each element tested in multiple phases (Bi, In, Sn, Sb), the one-to-one phase (in most cases, having a NiAs structure) displayed the highest activity in terms of onset potential, current density, and types of fuel oxidized. This observation coincides with previous results for PtRu alloy nanoscale blacks, which show that an equimolar ratio of Pt and Ru yielded the best performance for CO and HCOOH oxidation.[19] In the case of methanol it has been found that Pt-rich Pt−Ru alloys, with 10−30% Ru, are more suitable for the adsorption and oxidation of this fuel.[30−32] Electrode stability appeared to be enhanced by the Pt, as particularly Pt-poor materials ($PtSn_2$, $PtSn_4$, $Pt_3In_7$) readily dissolved at any potential, though it is too soon to conclude whether this effect was primarily driven by overall Pt content or by dilated nearest-neighbor Pt−Pt distances. Similarly, $PtIn_2$ and $PtSb_2$ were both

(30) Gasteiger, H. A.; Markovic, N. M.; Ross, P. N.; Cairns, E. J. *J. Phys. Chem.* **1993**, *97*, 12020.
(31) Gasteiger, H. A.; Markovic, N. M.; Ross, P. N.; Cairns, E. J. *J. Electrochem. Soc.* **1994**, *141*, 1795−1803.
(32) Gasteiger, H. A.; Markovic, N. M.; Ross, P. N.; Cairns, E. J. *Electrochim. Acta* **1994**, *39*, 1825−1832.

inactive and have nearest Pt−Pt distances of 4.501 and 4.555 Å, respectively. Most active phases have nearest-neighbor Pt−Pt distances of approximately 2.8 Å along one axis and greater than 4 Å in any other direction. These dilated Pt−Pt distances offer higher resistance to poisoning by CO. The chemical and electrochemical stability (potential window of stability) of intermetallic compounds was further studied and has been discussed in detail in another publication.[29]

The contention that formic acid can serve as a model fuel for candidate materials is now well-founded, as no material inactive to formic acid showed any activity toward any other fuel tested, and formic acid can be used with confidence as an initial screen for new intermetallic phases. It is hoped that ordered intermetallic phases afford enough control of surface characteristics to tailor a substrate to sufficiently enhance C−C bond cleavage so as to make ethanol and other C-2 SOMs viable fuels for fuel cell applications. Extensive efforts are underway to screen a broadened range of candidate materials to find superior electrocatalysts.

**Acknowledgment.** This work was supported by the Department of Energy and the National Science Foundation. E.C.-R. acknowledges support by a Provost's Diversity Fellowship from Cornell University. T.V.-A. thanks the Cornell Center for Materials Research REU Program of the summer of 2002 for support.

JA038497A